Journal of Photochemistry and Photobiology A: Chemistry 202 (2009) 48–56

Contents lists available at ScienceDirect

Journal of Photochemistry and Photobiology A: Chemistry

journal homepage: www.elsevier.com/locate/jphotochem

Photochemical and photophysical properties, and photodegradation mechanism, of the non-steroid anti-inflammatory drug Flurbiprofen

Klefah A.K. Musa, Leif A. Eriksson*

Department of Natural Sciences and Örebro Life Science Center, Örebro University, Fakultetsgatan 1, 701 82 Örebro, Sweden

ARTICLE INFO

Article history:
Received 10 June 2008
Received in revised form
14 September 2008
Accepted 17 November 2008
Available online 28 November 2008

Keywords:
Flurbiprofen
Photodegradation
Decarboxylation
NSAID
TD-DFT
Lipid peroxidation

ABSTRACT

The photodegradation mechanism of the widely used non-steroidal anti-inflammatory drug 2-(4-phenyl-3-fluorophenyl) propanoic acid, Flurbiprofen, and its photochemical and photophysical properties have been investigated by means of computational quantum chemistry at the DFT-B3LYP/6-31G(d,p) level. Comparison of computed and experimental singlet and triplet–triplet absorption spectra point to that most experiments, using a range of different solvents, are conducted on the neutral, protonated form of Flurbiprofen. The deprotonated acid, which should dominate at physiological pH, shows no sign of decarboxylation from the lowest singlet excited states, whereas from its first excited triplet state this should readily occur by passing over an energy barrier of <0.5 kcal/mol. Further reactions in the proposed photodegradation mechanism, after decarboxylation, as well as the probability for reactive oxygen species formation are discussed in detail. The generation of the corresponding peroxyl radical from the decarboxylated radical and molecular oxygen is strictly exergonic and occurs without barrier under aerobic conditions. The thus formed peroxyl radical will in turn be capable of initiating propagating lipid peroxidation processes.

1. Introduction

Flurbiprofen (FBP), S-2-(4-phenyl-3-fluorophenyl) propanoic acid, Scheme 1, belongs to arylpropionic acid derivatives which constitute the main group of non-steroidal anti-inflammatory drugs (NSAIDs), that in turn are among the most widely used therapeutic agents. FBP is a very potent NSAID widely used as an analgesic and antipyretic drug. It is also used in the treatment of acute gout [1], prevention of migraine headache [2], osteoarthritis [3,4], soft tissue injuries (tendinitis and bursitis) [5–7], rheumatoid arthritis [8], post-operative ocular inflammation [9], management of vernal keratoconjunctivitis [10], ocular gingivitis [11], herpetic stromal keratitis [12], and excimer laser photorefractive keratectomy [13]. In addition FBP has been suggested in the literature to be utilized in areas related to cancer management such as radio-protection [14], protection of post-irradiation myelosuppression [15], and inhibition of colon tumors [16]. FBP is also used in pain relief after foot surgery and periodontal surgery [17,18].

On the other hand, FBP has many adverse side effects. It can cause ulcerations, abdominal burning, pain, cramping, nausea, gastritis, drowsiness and stuffy nose. More severe side effects include chest pain, confusion, dark urine, depression, weakness, vision or speech changes, vomit that looks like coffee grounds, and yellowing of the skin or eyes [19]. Due to the presence of the biphenyl moiety the drug is highly lipid-soluble. It has thus been pointed out that, in addition to these side effects, FBP photoproducts formed in the skin after exposure to sunlight exert toxic side effects on cell membranes and causes noxious photoallergic contact dermatitis in clinical practice [20].

Pharmacologically, FBP is associated with inhibition of cyclooxygenase enzymes (COX-1 and COX-2, also referred to as prostaglandin H_2 synthases). These enzymes are responsible for the conversion of arachidonic acid into prostaglandin H_2, a key intermediate in the biosynthetic pathway of prostaglandins, prostacyclines and thromboxanes [21,22]. The mechanism of action of NSAIDs, as well their side effects, is largely explained by inhibition of prostaglandin synthesis of the COX enzyme isoforms. COX-1 is expressed in most tissues and cells and is abundant in the gastrointestinal tract, kidney, and platelets, whereas COX-2 is predominantly expressed in inflamed tissues. The main difference between these two isoforms is the active site amino acid at position 523; isoleucine in COX-1 and valine in COX-2. This slight modification contributes significantly to the COX-2 selectivity by opening up a second pocket in the active site [23]. FBP is a more potent inhibitor of prostaglandin biosynthesis than ibuprofen, indomethacin and aspirin, both *in vitro* and *in vivo* [24], but requires frequent dosage because of the short elimination half-life (3.9 h) [25]. Recently, it has been suggested that FBP also selectively inhibits the most toxic component of senile plaques present in the

* Corresponding author. Tel.: +46 19 303 652; fax: +46 19 303 566.
E-mail address: leif.eriksson@oru.se (L.A. Eriksson).

1010-6030/$ – see front matter © 2008 Elsevier B.V. All rights reserved.
doi:10.1016/j.jphotochem.2008.11.010

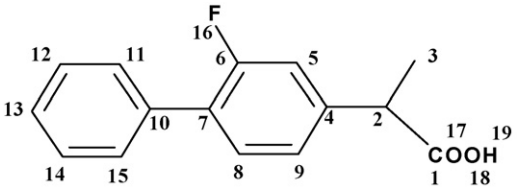

Scheme 1. Flurbiprofen (FBP) and the atomic numbering scheme used throughout the study.

brain of Alzheimer patients known as β-amyloid 42 (Aβ42) [26]. Worth noting is also that, although the pharmacological effect of FBP is mainly due to the S-enantiomer, it is usually sold as a racemic mixture [27]. The biological effects of the R-enantiomer are, to the best of our knowledge, not fully known.

Photosensitivity, phototoxicity, and photoallergic responses are among the most common side effects of NSAIDs, especially for the 2-arylpropionic acid derivatives. Drug-induced photosensitivity or phototoxicity is always related to the formation of photoproducts [28]. In order to prevent or minimize the side effects of gastrointestinal damage and the first-pass effect observed after oral administration due to COX-1 inhibition, topical application is often preferred, if possible, as it increases drug concentration in the tissue to which it is applied and reduces possible high levels in other tissues and blood. Topical application may, however, worsen the condition of photosensitivity, phototoxicity or photoallergic side effects. Drug-induced cutaneous photosensitivity to sunlight (UV or visible radiation) is a problem of much concern to dermatologists and the pharmaceutical industry [29].

FBP photodegradation intermediates and products have been investigated experimentally in a few studies. When FBP is irradiated in different solvents in the presence of oxygen, the corresponding alcohol and ketone forms were obtained when using organic solvents like methanol or hexane, whereas when phosphate buffer solution (PBS) is used as solvent the formation of the decarboxylated species dominates along with the ketone and a substituted phenol (*i.e.* substituting the fluorine atom to render 2-(4-phenyl-3-hydroxylphenyl) propanoic acid) formed through photonucleophilic aromatic substitution [30,31]. The photoreaction quantum yield has however been determined as relatively low (more than one order of magnitude less than for *e.g.* ketoprofen). The UV spectrum of FBP recorded experimentally in the wavelength regime between 200 and 400 nm shows a λ_{max} at 248 nm in aqueous sodium phosphate buffer (pH 6.4) and methanol–acetonitrile–phosphate buffer (pH 5.6), and a second major peak at around 220 nm [32]. In methanol–phosphate buffer, UV absorption at 254 nm was instead used to identify FBP [25]. It has also been noted, somewhat surprisingly, that there is no major change in neither the shapes of the peaks nor in the positions of the absorption maxima when methanol, hexane or acetonitrile is used as solvents [30], which implies that under the conditions used the molecule is either in the same protonation state, or that the different protonation states have very similar absorption spectra.

The molecule displays several decay mechanisms upon excitation. The fluorescence quantum yield for direct decay from the first excited singlet state ranges from 0.15 to 0.32 depending on solvent, with fluorescence lifetimes of the order 1–2 ns [30]. Alternatively the molecules can undergo intersystem crossing to the first triplet state. The intersystem crossing quantum yield is reasonably high, between 0.45 and 0.71, as determined through laser flash photolysis experiments. The triplet lifetimes range between 15 and 106 μs, with the highest value obtained in neutral aqueous buffer, and subsequent transient triplet–triplet absorption spectra could be observed with a broad peak centered at 360 nm [30]. The relatively short lifetimes of the excited singlet and triplet states have been interpreted as indicating deactivation through hydrogen bonding interactions involving the carboxylic groups.

In our previous theoretical studies concerning related 2-arylpropionic acid derivatives such as ketoprofen [33] and ibuprofen [34], their susceptibility to react with light (mainly UV radiation) has been explored in detail. The reactions are dependent on the concentration of the compound, the level of activating radiation, and the quantity of other chromophores in the skin. Absorption of radiation produces an excited-state compound or metabolite, which in turn may follow one of two pathways that lead to photosensitization, involving either the generation of a free radical or singlet oxygen. These will, in turn, result in the oxidation of biomolecules, damaging critical cellular components and initiating the release of erythrogenic mediators [35,36].

Based on the experimental studies of FBP a decarboxylation mechanism based on the first excited singlet state has been proposed [30,31]. Based on our previous theoretical studies of NSAIDs mentioned above [33,34], we have in the current work explored this possibility, and also constructed and studied a photodegradation mechanism following the triplet route (as this is more common for NSAIDs) as displayed in Scheme 2. Deeper insight on the physicochemical properties of this compound will in turn assist in the design of new drugs with less harmful side effects. The theoretical studies are furthermore a valuable tool in understanding the mechanism of action of the compound. We have in the current work explored the possible photoinduced decarboxylation of FBP, and subsequent reactions leading to the generation of reactive oxygen species and initiators of lipid peroxidation reactions.

2. Methodology

All geometries of FBP, its radical anion, radical cation, anionic form and decarboxylated forms, as well as intermediates in the photodegradation process, were optimized at the hybrid Hartree-Fock–Density Functional Theory B3LYP/6-31G(d,p) level [37–39]. Solvent effects were taken into consideration implicitly, through single point calculations on the optimized geometries at the same level of theory including the integral equation formulation of the polarized continuum model (IEFPCM) [40–42]. Water was used as solvent, through the value 78.31 for the dielectric constant in the IEFPCM calculations. Frequency calculations were performed on the optimized geometries at the same level of theory *in vacuo*, to ensure the systems to be local minima (no imaginary vibration frequencies), and to extract zero-point vibrational energies (ZPEs) and thermal corrections to the Gibbs free energies at 298 K. Excitation spectra were calculated using the time-dependent formalism (TD-DFT) [43–45], at the same level of theory. The numbering scheme of the atoms used throughout the study is given in Scheme 1. All calculations were performed using the Gaussian 03 programme package [46].

3. Results and discussion

3.1. Redox chemistry of Flurbiprofen

We begin by investigating the redox properties of the FBP parent compound **A**. The optimized structures of FBP, its radical anion and radical cation ($\mathbf{A}^{\bullet -}$ and $\mathbf{A}^{\bullet +}$), and its deprotonated form $\mathbf{A}^{-}$ are displayed in Fig. 1. In the optimized structures, the main difference is a change in the C_1–C_2 bond length which is responsible for decarboxylation, from 1.524 Å in neutral from (a) to 1.607 Å in the deprotonated structure (d). However, very little change in this bond length is seen for both the radical anion and the radical cation (b and c) compared with the protonated structure. In these, the notable dif-

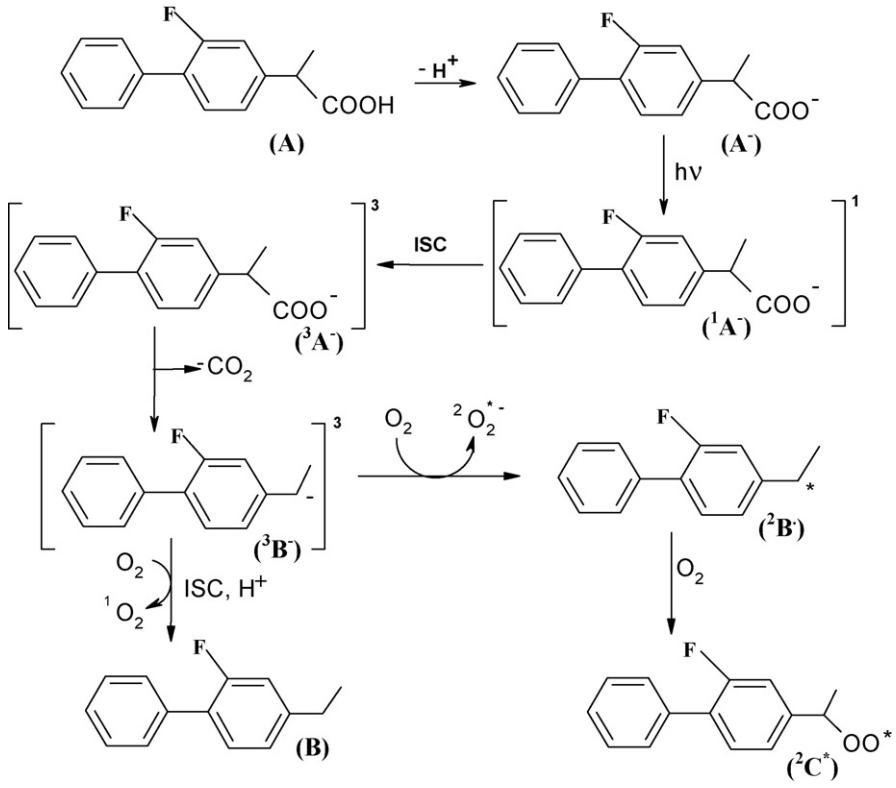

Scheme 2. Proposed mechanism of FBP photodegradation.

ference is instead a shortening of the length of the biphenyl bridge (C_7–C_{10}).

The absolute and relative ZPE-corrected energies in the gas phase and in bulk solution, along with dipole moments obtained in aqueous solution, are listed in Table 1. The electron affinity (EA) and ionization potential (IP) of FBP obtained from the calculated energies amount in gas phase to −3.7 and 173.5 kcal/mol, respectively. The negative EA of the anionic species implies that the anion radical in this case is unstable. Applying a bulk solvent through the IEFPCM method, we instead obtain the values 34.3 and 135.9 kcal/mol for EA and IP, respectively.

In the gas phase, the energy difference between the protonated and the deprotonated species is 346.4 kcal/mol which is reduced to 295.1 kcal/mol in aqueous solution. These data are highly

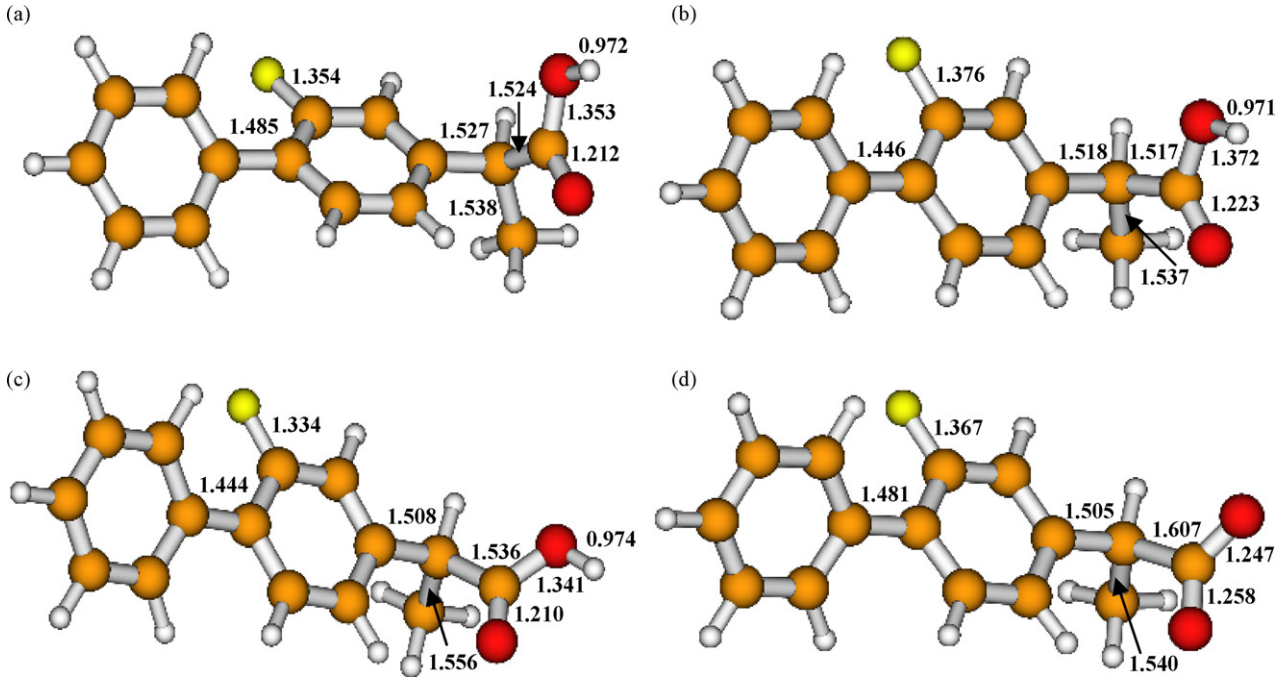

Fig. 1. B3LYP/6-31G(d,p) optimized structures of (a) neutral ground state FBP (**A**); (b) radical anion ($\mathbf{A}^{\bullet -}$); (c) radical cation ($\mathbf{A}^{\bullet +}$); (d) deprotonated form ($\mathbf{A}^{-}$).

Table 1
B3LYP/6-31G(d,p) ZPE-corrected electronic energies of FBP in gas phase, and IEFPCM-B3LYP/6-31G(d,p) Gibbs free energies in aqueous solution.

System	$E_{(ZPE)}$	$\Delta E_{(ZPE)}$	$\Delta G_{aq}{}^{298}$	$\Delta\Delta G_{aq}{}^{298}$	μ_{aq}
^{1}**A**	−829.513191	0	−829.575129	0	0.85
^{2}**A**$^{\bullet-}$	−829.507258	3.7	−829.629801	−34.3	4.96
^{2}**A**$^{\bullet+}$	−829.236682	173.5	−829.358552	135.9	4.64
^{3}**A**	−829.407098	66.6	−829.471754	64.9	0.65
^{1}**A**$^-$	−828.961217	346.4	−829.104924	295.1	19.44
^{3}**A**$^-$	−828.87453	400.8	−828.998728	361.7	11.38
^{3}**B**$^-$	−640.301809	0	−640.414135	0	4.28
^{1}**B**$^-$	−640.360957	−37.1	−640.470662	−35.5	4.64
^{1}**B**	−640.960125	−413.1	−641.006307	−371.6	1.90
^{2}**B**$^\bullet$	−640.327229	−16.0	−640.375423	24.3	2.28
^{2}**C**$^\bullet$	−790.669821	–	−790.725363	–	2.96

Absolute energies in a.u., relative energies in kcal/mol. Dipole moments μ (D) in aqueous solution.

similar (to within ∼10 kcal/mol) to those obtained for the other related non-steroidal anti-inflammatory compounds (ketoprofen and ibuprofen) previously investigated [33,34].

The Mulliken atomic charge distributions of the various molecules are displayed in Table 2. The local charge on the carboxylic moiety (O_{17}–C_1–O_{18}–(H_{19})) of the neutral parent compound and its radical anion, radical cation and deprotonated counterparts are −0.043, −0.174, 0.040 and −0.929 e$^-$, respectively, in line with the computed dipole moment of these species displayed in Table 1. We note a change by ∼4 D between the parent compound and its radical anion or radical cation, whereas for the deprotonated acid the dipole moment increases by more than 18 D due to the highly localized negative charge. For the decarboxylated species in the photodegradation mechanism, the Mulliken atomic charges are localized mainly on C_3 of the α-methyl moiety, on C_6 of the first aromatic ring connected to F_{16}, and on the fluorine atom (cf. Table 2).

The unpaired electron density (Table 3) is in the radical anion and radical cation localized to atoms C_4 and C_7 of the central phenyl ring, that connects to the propanoic acid moiety and to the other phenyl ring, respectively, and on C_{13} and C_{15} of the second phenyl ring. In the radical anion (radical cation), the spin densities on atoms C_4, C_7, C_{13} and C_{15} are 0.257 (0.236), 0.157 (0.165), 0.216 (0.266) and 0.125 (0.110) e$^-$, respectively. For the decarboxylated moieties (^{3}**B**$^-$ and ^{2}**B**$^\bullet$), the main portion of the unpaired spin density is localized to C_2 (connected to the carboxylic moiety in the parent molecule), whereas for the corresponding peroxyl radical ^{2}**C**$^\bullet$ the spin density localized mainly on the –OO$^\bullet$ group.

A study of the molecular orbital configurations of the compound leads to further insights into its photochemistry. In Fig. 2 we display the computed highest occupied and lowest unoccupied molecular orbitals (HOMOs and LUMOs, respectively) of neutral and deprotonated FBP. The HOMO of the protonated species is delocalized over both aromatic rings, whereas HOMO-1 is localized only on the peripheral aromatic ring and HOMO-2 only on the central ring. For the deprotonated acid, the three highest occupied molecular orbitals are localized mainly to the carboxylic moiety of the propionic group. This can be inferred by looking at the Mulliken atomic charge distribution on the carboxylic group, where the neutral form holds only −0.043 e$^-$ while the deprotonated species is accounted for −0.929 e$^-$ on the same moiety. The LUMO of the neutral form is delocalized over almost the entire molecule, whereas the LUMO + 1 is centered on the substituted phenyl ring, and LUMO + 2 on the peripheral aromatic ring. For the deprotonated form, LUMO also delocalized although more centered on the peripheral aromatic ring, LUMO + 1 is fully localized on the peripheral phenyl ring, and LUMO + 2 on the central substituted aromatic ring only. Excitation of the deprotonated species can hence be expected to render large charge re-distributions in the molecule.

3.2. Excitation of Flurbiprofen and its deprotonated species

The initial step in the photodegradation of FBP is the excitation of **A** in its neutral or deprotonated form to the first excited singlet state S_1 (or a higher lying singlet S_n followed by radiationless decay to S_1). Experimentally, decarboxylation is proposed to occur already from the S_1 state [30,31], whereas the mechanism outlined in Scheme 2 assumes the system to undergo intersystem crossing (ISC) to the first excited triplet state. Since the pK_a value of FBP is low (4.27) [47,48], it will predominantly exist in its deprotonated (acidic) form at physiological pH; *i.e.* photodegradation can be expected to occur primarily from **A**$^-$. In Fig. 3, we display the computed spectra of the neutral and deprotonated forms of FBP. Although the two spectra display clear differences, they both have very clear absorption

Table 2
Mulliken atomic charges (B3LYP/6-31G(d,p) level) on selected atoms of FBP.

System	C_1	C_3	C_6	F_{16}	O_{17}	O_{18}	H_{19}
^{1}**A**	0.59	−0.299	0.311	−0.294	−0.468	−0.487	0.322
^{2}**A**$^{\bullet-}$	0.563	−0.293	0.273	−0.331	−0.521	−0.511	0.295
^{2}**A**$^{\bullet+}$	0.596	−0.318	0.365	−0.243	−0.443	−0.460	0.347
^{3}**A**	0.589	−0.301	0.328	−0.286	−0.469	−0.488	0.322
^{1}**A**$^-$	0.290	−0.297	0.290	−0.320	−0.609	−0.610	–
^{3}**A**$^-$	0.288	−0.306	0.288	−0.319	−0.509	−0.517	–
^{1}**B**$^-$[a]	–	−0.321	0.287	−0.337	–	–	–
^{3}**B**$^-$[b]	–	−0.333	0.274	−0.329	–	–	–
^{1}**B**	–	−0.308	0.31	−0.296	–	–	–
^{2}**B**$^\bullet$	–	−0.357	0.313	−0.297	–	–	–
^{2}**C**$^\bullet$	–	−0.317	0.313	−0.291	–	–	–

For atomic labeling, see Scheme 1.

[a] C_2 = −0.246, C_4 = 0.217, C_5 = −0.240.

[b] C_5 = −0.210.

Table 3
Atomic spin densities (B3LYP/6-31G(d,p) level) on selected atoms for the open shell species of FBP.

System	C_2	C_4	C_6	C_7	C_8	C_{13}	C_{15}
^{2}**A**$^{\bullet-}$		0.257	0.032	0.157	0.125	0.216	0.125
^{2}**A**$^{\bullet+}$		0.236	0.132	0.165		0.266	0.110
^{3}**A**		0.533	0.241	0.257	0.260	0.507	0.307
^{3}**A**$^-$		0.335	0.037	0.319		0.349	0.229
^{3}**B**$^-$	0.788		−0.051	0.243		0.337	
^{2}**B**$^\bullet$	0.736		−0.114	0.255			
^{2}**C**$^\bullet$	For –OO group connected at C_2, O_{inner} = 0.299, O_{outer} = 0.695						

For atomic labeling, see Scheme 1.

peaks in the 260–270 nm range. The spectrum of the deprotonated form indicates that the molecule should also be able to absorb light in the visible region (around 480 nm). Comparing with the experimental spectra recorded under different conditions [25,30,32], it appears that what has been detected experimentally is the neutral (protonated) species also in sodium phosphate buffer, and not the deprotonated compound. The UV spectrum between 200 and 400 nm in PBS solution displays two clear peaks at 220 and 248 nm, with a relative intensity ratio of 3:1 [25,32,48]; in perfect agreement with the current results for the neutral species taking into account that the current methodology blue-shifts the absorptions by approximately 10–15 nm in the current wavelength regime.

For the neutral (protonated) species, the computed first vertical excitation (HOMO → LUMO) occurs at λ = 262 nm, in the UV-regime of the spectrum, with oscillator strength f = 0.436, followed by an absorption at λ = 247 nm (f = 0.120). The other major peaks of **A** are found at λ = 187 nm (f = 0.727), λ = 168 nm (f = 0.123), and λ = 164 nm (f = 0.398).

For the deprotonated species $\mathbf{A}^-$, the $S_0 \rightarrow S_1$ excitation is found at λ = 493 nm with relatively with low probability (f = 0.044) followed by an absorption at λ = 478 nm (f = 0.101). The main peak is found at λ = 274 nm (f = 0.294), i.e. at slightly longer wavelength than the corresponding one obtained for the neutral form. This gives further indication for the hypothesis that the experimental studies, according to which there is no major change in the positions or the shape of the absorption peaks from 200 to 380 nm when methanol, hexane or acetonitrile are employed as solvents [30], are conducted on the neutral form of FBP. Other major peaks of the deprotonated acid are noted at λ = 257 nm (f = 0.143) and λ = 218 nm (f = 0.055). Overall, the excitations within the acid have relatively speaking

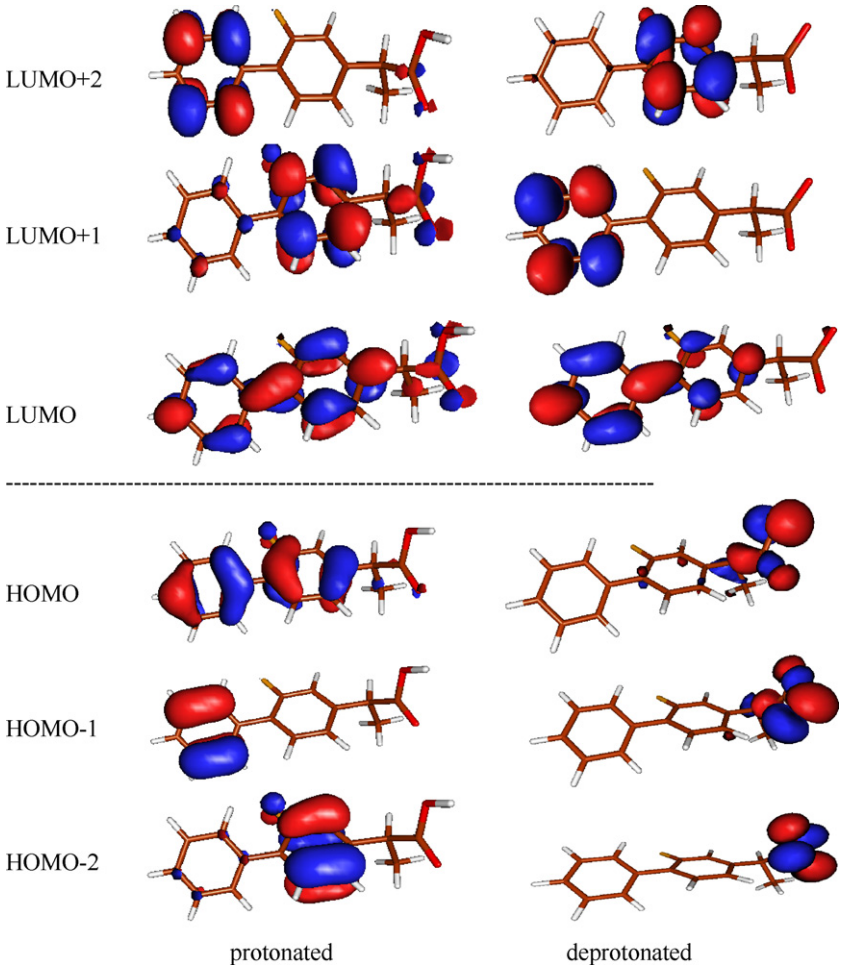

Fig. 2. Molecular orbitals of FBP. Neutral (protonated) to the left and deprotonated anion to the right.

lower probabilities than the absorptions in the neutral system. This is due to the charge-transfer (CT) nature and thus low overlap of involved MOs, as we transfer an electron from the carboxylic moiety into the ring system (cf. Fig. 2).

Energetically, the initial $S_0 \rightarrow S_1$ excitation requires 58 kcal/mol for the deprotonated system, following intersystem crossing to the T_1 state that will relax to a free energy 54.4 kcal/mol above S_0. For the neutral form the $S_0 \rightarrow S_1$ excitation requires 108 kcal/mol, in good agreement with experimental value 99 kcal/mol of the neutral species [30], taking into account the slight overestimation of excitation energies (in most cases around 5 kcal/mol) obtained with this computational method. A low yield of photodegradation products was reported experimentally, along with a transient species with a triplet–triplet excitation spectrum displaying a broad peak centered at 360 nm. In Fig. 3B we display the triplet–triplet excitations of the neutral species, the deprotonated form, and the decarboxylated anion. A large absorption peak centered at 360 nm matches perfectly the triplet–triplet spectrum computed for the neutral FBP. Taken together, the difference between theoretical and experimental data *in vitro* implies that the system studied experimentally is for the most parts the neutral molecule, and not the deprotonated, or decarboxylated, species. Most likely, the solvent plays a crucial role in modifying the properties of the acid.

As FBP is a substituted arylpropionic acid that will exist predominately in the deprotonated form at physiological pH, photodegradation is expected to occur with decarboxylation as the dominant initial degradation process (bearing in mind the high quantum yields of deactivation of the excited states), and where radical formation after decarboxylation can also be expected. The optimized triplet state of the deprotonated form ($^3\mathbf{A}^-$) lies 54 kcal/mol above the optimized ground state $\mathbf{A}^-$; for the protonated species, the corresponding free energy difference is 67 kcal/mol. The values are affected very little by the inclusion of bulk solvation. The energy of the first excited triplet of the optimized neutral species agrees very well with the corresponding experimental data reporting the $S_0 \rightarrow T_1$ energy to be close to 65 kcal/mol [30]. The vertical T_1 energies obtained from TD-DFT calculations of the deprotonated and neutral species also agree with these values (52 kcal/mol and 73 kcal/mol, respectively), indicating that there is relatively little structural relaxation of the T_1 state. The triplet excitation lifetimes of neutral FBP in deaerated media were found to be between 15 and 106 μs, depending on solvent, with intersystem crossing quantum yields ranging between 0.45 and 0.71 [30].

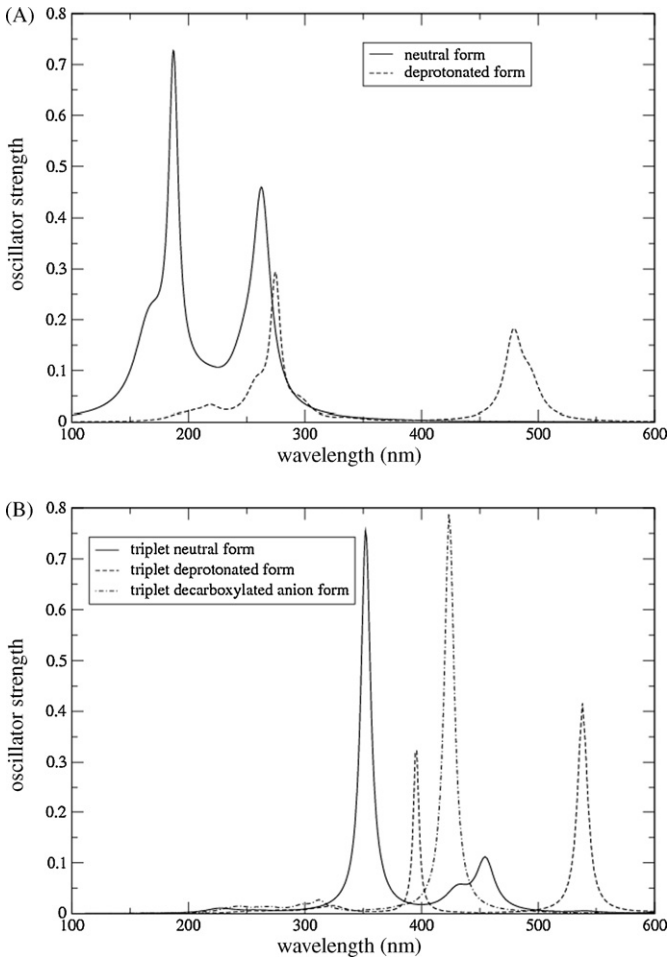

Fig. 3. Computed absorption spectra of (A) the neutral (solid) and deprotonated (dashed) forms of FBP and (B) triplet–triplet excitation spectra of the neutral (solid), deprotonated (dashed) and decarboxylated product $^3\mathbf{B}^-$ (dot-dashed) of FBP, obtained at the TD-B3LYP/6-31G(d,p) level.

The optimized structures of the triplet states of the neutral and deprotonated species are shown in Fig. 4. For the neutral (protonated) form, very small changes in geometry are noted, compared to the singlet ground state. This provides further support for the high photostability of the T_1 state observed experimentally. In the deprotonated species, the main structural change is a considerable elongation of the C_1–C_2 bond length from 1.607 Å in the singlet ground state to 1.779 Å in the triplet state (i.e. very close to dissociation leading to decarboxylation). The situation is in this case highly similar to ibuprofen [34] but different from the case of ketoprofen, for which the deprotonated triplet state undergoes spontaneous decarboxylation [33].

The unpaired spin components of the optimized deprotonated and (protonated) triplet state structures are mainly distributed on C_4, C_7, C_{13}, and C_{15}, with values 0.335 (0.533), 0.319 (0.257), 0.349 (0.507), and 0.229 (0.307) e^-, respectively. A negative charge of approximately −0.738 e^- is located on the carboxyl moiety of FBP in the optimized deprotonated triplet, while only −0.046 e^- is located on the same group in the neutral case. This can again be rationalized from the difference between the HOMO and LUMO of the two forms (neutral and deprotonated). Comparing with the ground-state acid, a charge of −0.929 e^- was observed on the carboxylic moiety. Upon excitation from HOMO to LUMO, more of the electron distribution is moved from the carboxylic group into the phenylic rings (cf. Fig. 2); hence the reduced charge. For the neutral triplet to deprotonate requires 296.8 kcal/mol, which is very similar to that of the singlet state deprotonation (295.1 kcal/mol).

In order to investigate whether decarboxylation can occur from an excited singlet state of the deprotonated acid, the C_1–C_2 bond was scanned outward from the optimized S_0 value (1.607 Å) in steps of 0.1 Å. In each new point, the structures were re-optimized, and the vertical excitation energies calculated. The resulting energy curves, obtained at the TD-B3LYP/6-31G(d,p) level, are displayed in Fig. 5, including several of the lowest singlet excited states. The ground and most of the lowest excited singlet state surfaces are strictly endothermic throughout the scan, and hence show no sign of decarboxylation. The exception is the S_4 state (and possibly S_7), which displays an apparent transition barrier with a maximum at a C_1–C_2 distance of ∼2.2 Å. The barrier to decarboxylation is rather high (around 21 kcal/mol), and it can thus be concluded that decarboxylation is not likely to occur from the excited singlet states of the FBP anion. This condition is very similar to the behavior found for ibuprofen [34]. As noted above for the triplet structures, this situation is also markedly different from the case of ketoprofen, for which several of the singlet excited states of the deprotonated form would lead to decarboxylation by overcoming a barrier of only a few kilocalories per mole [33]. Again, the current findings for FBP are in excellent agreement with experimental data, which show that

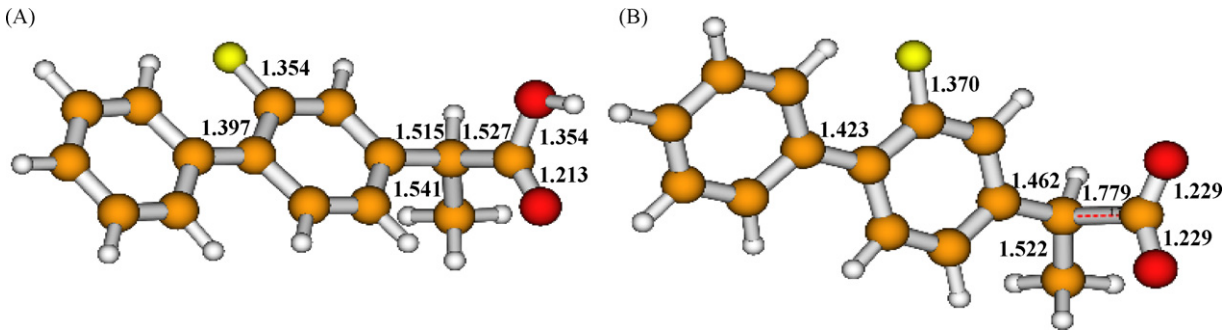

Fig. 4. Optimized structures (B3LYP/6-31G (d,p) level) of (A) neutral and (B) deprotonated T_1 states of FBP.

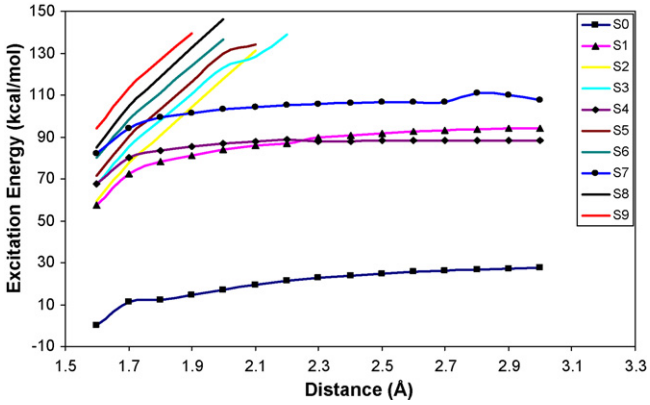

Fig. 5. Energy curves for decarboxylation of deprotonated FBP, including the ground state and several of the lowest excited singlet states.

the quantum yield for decarboxylation is less than 0.01 in PBS and organic solvents. As the molecule appears from the spectroscopic data to be predominantly in the protonated state, photoinduced decarboxylation will indeed be a minor reaction as it is not likely to occur from a neither singlet or a triplet excited state of neutral FBP, nor from the excited singlet anion [30].

Due to the elongation of the C_1–C_2 bond length by 0.17 Å in the optimized triplet state of the deprotonated form compared to the S_0 state (Fig. 4), this bond was scanned in the same manner as described above in order to determine the energy barrier for decarboxylation. The energy barrier for decarboxylation from the triplet state is only about 0.4 kcal/mol, and occurs at a TS of C_1–C_2 distance approximately 2.1 Å as shown in Fig. 6. This can be compared again with the corresponding processes in ketoprofen and ibuprofen; for the former, decarboxylation from the triplet state occurs spontaneously upon formation, while for the latter the result is similar to that of obtained for FBP (energy barrier 0.3 kcal/mol and C_1–C_2 distance 1.97 Å) [33,34].

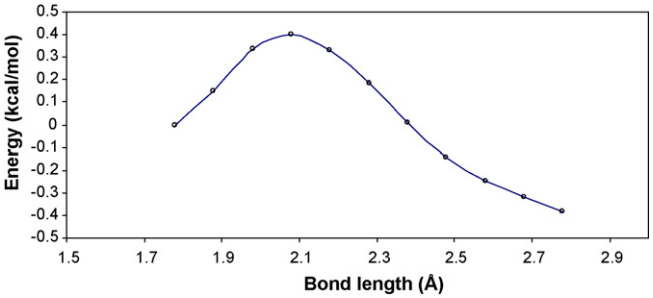

Fig. 6. Energy barrier for decarboxylation from the first excited triplet state of deprotonated FBP.

3.3. The fate of decarboxylated Flurbiprofen

From the findings described above, the decarboxylation of deprotonated species of FBP is not likely to occur from singlet excited states, but should occur to a high degree from the triplet state due to the high $Ø_{ISC}$ (between 0.45 and 0.71) and low energy barrier (0.4 kcal/mol). This leads to various subsequent photoreactions as depicted in Scheme 2, and can be summarized as follows (reactions (1)–(3)).

$$^3\mathbf{A}^- \xrightarrow{-CO_2} {}^3\mathbf{B}^- \xrightarrow[O_2]{ISC,H^+} \mathbf{B} + {}^1O_2 \quad (1)$$

$$^3\mathbf{A}^- \xrightarrow{-CO_2} {}^3\mathbf{B}^- \xrightarrow{O_2} {}^2\mathbf{B}^\bullet + {}^2O_2{}^{\bullet-} \quad (2)$$

$$^2\mathbf{B}^\bullet \xrightarrow{O_2} {}^2\mathbf{C}^\bullet(=\mathbf{BOO}^\bullet) \quad (3)$$

According to reaction (1), the triplet state of the 4-phenyl-3-fluorophenylethane anion $^3\mathbf{B}^-$ is formed from $^3\mathbf{A}^-$ after decarboxylation. Optimization of this species in its singlet and triplet forms shows that the triplet lies about 37 kcal/mol above the singlet state. Inclusion of bulk solvation effect reduces this value to 35.5 kcal/mol. The triplet state has one of its unpaired electrons localized on C_2 (spin density 0.788 e^-), and the other delocalized on the rings. Upon ISC and protonation, neutral 4-phenyl-3-fluorophenylethane will be formed. During this process, singlet oxygen formation can be expected in the ISC process. The excitation energy of ground state molecular oxygen leading to the formation of singlet oxygen is 22.5 kcal/mol [49] compared with the 36 kcal/mol energy difference between the triplet and singlet forms of $\mathbf{B}^-$. $^1\mathbf{B}^-$ can be expected to protonate more or less instantaneously because of its very high proton affinity, around 336 kcal/mol in aqueous solution. The absorption spectrum of the decarboxylated species $^3\mathbf{B}^-$ was also calculated, and is displayed in Fig. 3B. The calculated spectrum shows one dominant peak at $\lambda = 424$ nm with oscillator strength $f = 0.789$, in addition to a couple of transitions with very low intensity in the UV region ($f < 0.05$) not likely to be detectable, and could serve as help in detection of the decarboxylated species. The triplet–triplet absorption spectrum of $^3\mathbf{B}^-$ is markedly different from the neutral and anionic carboxylated parent compounds.

Reaction (2) shows another possible fate of $^3\mathbf{B}^-$ in which electron transfer to molecular oxygen occurs, and generates superoxide radical anions. Due to the large stabilization of the charged form by the polar solvent, the anion is 24.3 kcal/mol more stable than its radical form $^2\mathbf{B}^\bullet$ (Table 1). This should be compared with the adiabatic electron affinity of molecular oxygen to generate superoxide in solution, estimated to 90.2 kcal/mol (3.91 eV) [50], which implies that the overall reaction will be exergonic by approximately 66 kcal/mol. In the cases of ketoprofen and ibuprofen, the corresponding processes were exothermic by 27 and 77 kcal/mol, respectively [33,34]. Under aerobic condition in polar media, irreversible quenching of

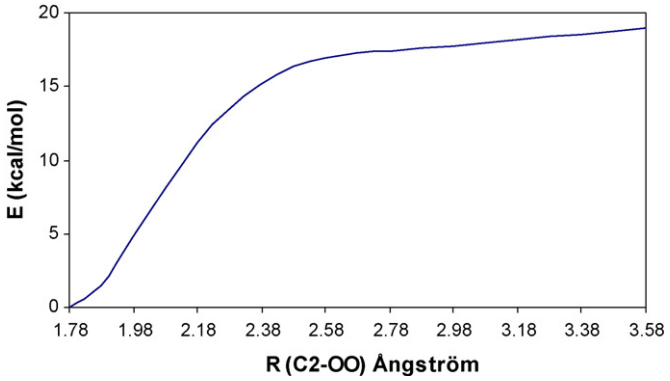

Fig. 7. Reaction path for the formation of peroxyl radical $^{2}\mathbf{C}^{\bullet}$ from $^{2}\mathbf{B}^{\bullet}$ and molecular oxygen.

the triplet anion by oxygen-dependent electron transfer can hence be expected to lead to 4-phenyl-3-fluorophenylethane radical $^{2}\mathbf{B}^{\bullet}$ and superoxide anion formation.

The addition of molecular oxygen in its $^{3}\Sigma$ ground state to the 4-phenyl-3-fluorophenylethane radical $^{2}\mathbf{B}^{\bullet}$ will generate the peroxyl radical $^{2}\mathbf{C}^{\bullet}$ (reaction (3)). As expected, $^{2}\mathbf{B}^{\bullet}$ has its unpaired spin density mainly located at C_2 (0.736 e^{-}), and thus makes an efficient target to attack by molecular oxygen. This reaction was explored by scanning the C_2–OO distance in steps of 0.1 Å; the energy diagram for this process is displayed in Fig. 7. The energy difference between the peroxyl radical product $^{2}\mathbf{C}^{\bullet}$ and that where the two reactants are separated by 3.5 Å, is 19 kcal/mol. The reaction is strictly exothermic with a clear change in slope at a C–O distance around 2.4 Å. The generation of the peroxyl radical is thus also strictly exergonic under aerobic conditions; in the presence of molecular oxygen reaction (3) will occur spontaneously and without any barrier.

Compound $^{2}\mathbf{C}^{\bullet}$, resulting from reaction (3), has a highly lipid-soluble biphenyl moiety. If this compound is embedded in a biological membrane, it will readily abstract a hydrogen from a lipid molecule, which through addition of molecular oxygen to the lipid radical site $\mathbf{L}^{\bullet}$ creates a propagating radical damage; reactions (4)–(6). Once initiated, the chain reactions (5) and (6) will repeat until terminated by *e.g.* radical–radical addition or the action of antioxidants such as vitamin E. The ease of formation of the peroxyl radical upon excitation of $\mathbf{A}^{-}$ and subsequent reactions explains the (in relative terms) abundant contact dermatitis observed for FBP [20].

$$^{2}\mathbf{BOO}^{\bullet}(=^{2}\mathbf{C}^{\bullet}) \rightarrow \mathbf{B(OOH)} + \mathbf{L}^{\bullet} \quad (4)$$

$$\mathbf{L}^{\bullet} + \mathbf{O}_2 \rightarrow \mathbf{LOO}^{\bullet} \quad (5)$$

$$\mathbf{LOO}^{\bullet} + \mathbf{LH} \rightarrow \mathbf{LOOH} + \mathbf{L}^{\bullet} \quad (6)$$

4. Concluding remarks

The proposed photodegradation mechanism of FBP and its photochemical properties were investigated theoretical by means of density functional theory at the B3LYP/6-31G(d,p) level. The computed absorption spectra of the neutral, deprotonated and decarboxylated species were obtained by TD-DFT methodology at the same level. The optimized structures of the different species show that the C_1–C_2 bond length elongates by about 0.1 Å by deprotonating the acid. Further extension of this bond by about 0.18 Å is noted in the optimized first excited triplet state of the deprotonated form. The deprotonation free energy in bulk solvation (295 kcal/mol) agrees with the experimental pK_a value of 4.27, showing that the compound will be deprotonated under physiological pH. The calculated spectrum of the deprotonated species has its main peak at $\lambda = 274$ nm ($f = 0.294$). This peak lies a longer wavelengths than that obtained for the main peak of the neutral form. Taken together with the triplet–triplet absorption spectra, the current findings imply that the *in vitro* experiments using different solvents are most likely conducted on the neutral, and not the deprotonated, acid.

The computed energies show that the deprotonated form will not be able to decarboxylate from the singlet excited states since the ground and most of the lowest singlet excited state surfaces for C_1–C_2 dissociation (decarboxylation) are strictly endothermic. The possibility of the neutral species to decarboxylate from the excited singlet will be far less, which agrees with the low experimental quantum yield of decarboxylation from the first excited singlet state (<0.01). Instead, decarboxylation will occur with very high efficiency from its first excited triplet state of the deprotonated species, which is reached through ISC from the excited singlet. The energy barrier for decarboxylation of the deprotonated species is in this case less than 0.5 kcal/mol. This is also in accordance with the experimental data; the quantum yield for singlet to triplet ISC of the neutral species, Φ_{ISC}, is between 0.45 and 0.71, but very little photoproducts are seen [30]. Hence, besides the fraction that fluoresces directly down to S_0 from an excited singlet state, also the neutral species will lead to triplet formation once excited, but as this is very stable towards decarboxylation (cf. Fig. 4) it will decay to the ground state rather than photodegrade.

A number of photoreactions occur subsequent to decarboxylation of the anionic species. The triplet anion of 4-phenyl-3-fluorophenylethane, $^{3}\mathbf{B}^{-}$, may convert to its ground state by ISC and proton addition, generating singlet oxygen. The superoxide radical anion can be formed during formation of the doublet state of 4-phenyl-3-fluorophenylethane, which in turn reacts with a second molecule of oxygen leading to the corresponding peroxyl radical. The generation of the peroxyl radical is strictly exergonic and occurs spontaneously and without any barrier under aerobic conditions.

Acknowledgements

The MENA programme (KAKM), the Swedish Science Research Council and the Faculty of Science and Technology at Örebro University (LAE) are gratefully acknowledged for financial support. We also acknowledge generous grants of computing time at the National Supercomputing Center (NSC) in Linköping.

References

[1] P.L. Lomen, L.F. Turner, K.R. Lamborn, M.A. Winblad, R.L. Sack, E.L. Brinn, Am. J. Med. 80 (1986) 134–139.
[2] G.D. Solomon, R.S. Kunkel, Cleveland Clin. J. Med. 60 (1993) 43–48.
[3] N.P. Misra, J. Postgrad. Med. 38 (1992) 164–166.
[4] N. Bellamy, W.G. Bensen, P.M. Ford, S.H. Huang, J.Y. Lang, Clin. Invest. Med. Med. Clin. Exp. 15 (1992) 427–433.
[5] R.A. Moore, M.R. Tramer, D. Carroll, P.J. Wiffen, H.J. Mcquay, Brit. Med. J. 316 (1998) 333–338.
[6] D.S. Muckle, Am. J. Med. 80 (1986) 76–80.
[7] H.R. Mena, P.L. Lomen, L.F. Turner, K.R. Lamborn, E.L. Brinn, Am. J. Med. 80 (1986) 141–144.
[8] J. Rovensky, D. Micekova, Drugs Exp. Clin. Res. 26 (2000) 19–24.
[9] M. Diestelhorst, B. Schmidl, W. Konen, U. Mester, P.S. Raj, J. Cataract Refract. Surg. 22 (Suppl. 1) (1996) 788–793.
[10] R.N. Sud, R.S. Greval, R.S. Bajwa, Ind. J. Med. Sci. 49 (1995) 205–209.
[11] D.S. Jones, C.R. Irwin, A.D. Woolfson, J. Djokic, V. Adams, J. Pharm. Sci. 88 (1999) 592–598.
[12] R.B. Vajpayee, B.P. Dhakal, S.K. Gupta, M.S. Sachdev, G. Satpathy, S.G. Honavar, A. Panda, Aust. N. Z. J. Opthamol. 24 (1996) 131–135.
[13] A. Appiotti, L. Gualdi, M. Alberti, M. Gualdi, Clin. Ther. 20 (1998) 913–920.
[14] M. Hofer, M. Pospisil, I. Pipalova, Folia Biol. (Prague) 42 (1996) 267–269.
[15] L. Juchelkova, M. Hofer, M. Pospisil, I. Pipalova, Physiol. Res./Acad. Sci. Bohemoslov. 47 (1998) 73–80.
[16] J.D. McCracken, W.J. Wechter, Y. Liu, R.l. Chase, D. Kantoci, E.D. Murray Jr, D.D. Quiggle, Y. Mineyama, J. Clin. Pharm. 36 (1996) 540–545.
[17] U. Bragger, T. Muhle, L. Fourmousis, N.P. Lang, A. Mombelli, J. Periodontal Res. 32 (1997) 575–582.

[18] S.M. Soulier, J.C. Page, L.C. Larsen, B.C. Grose, J. Foot Ankle Surg. 36 (1997) 414–417.
[19] http://www.drugs.com/sfx/flurbiprofen-side-effects.html.
[20] A. Kawada, Y. Aragane, A. Maeda, T. Yudate, T. Tezuka, Contact Dermat. 42 (2000) 167–168.
[21] C.I. Bayly, W.C. Black, S. Leger, N. Ouimet, M. Ouellet, M.D. Percival, Bioorg. Med. Chem. Lett. 9 (1999) 307–312.
[22] T. Smith, J. McCracken, Y. Shin, D. DeWitt, J. Biol. Chem. 275 (2000) 40407–40415.
[23] W.F. Hood, J.K. Gierse, P.C. Isakson, J.R. Kiefer, R.G. Kurumbail, K. Seibert, J.B. Monahan, Mol. Pharmacol. 63 (2003) 870–877.
[24] R.N. Hogden, R.C. Heel, T.M. Speight, G.S. Avery, Drugs 18 (1979) 417–438.
[25] N.A. Charoo, A.A.A. Shamsher, K. Kohli, K.K. Pillai, Z. Rahman, Chromatographia 62 (2005) 493–497.
[26] L. Peretto, S. Radaelli, C. Parini, M. Zandi, L.F. Raveglia, G. Dondio, L. Fontanella, P. Misiano, C. Bigogno, A. Rizzi, B. Riccardi, M. Biscaioli, S. Marchetti, P. Puccini, S. Catinella, L. Rondelli, V. Cenacchi, T. Bolzoni Pier, P. Caruso, G. Villetti, F. Facchinetti, E. Del Giudice, N. Moretto, B.P. Imbimbo, J. Med. Chem. 48 (2005) 5705–5720.
[27] A.M. Evans, J. Clin. Pharmacol. 36 (1996) 7S–15S.
[28] D.E. Moore, Drug Safety 25 (2002) 345–372.
[29] B.E. Johnson, J. Ferguson, Semin. Dermatol. 9 (1990) 39–46.
[30] M.C. Jimenez, M.A. Miranda, R. Tormos, I. Vaya, Photochem. Photobiol. Sci. 3 (2004) 1038–1041.
[31] S. Chao, H. Ho, F. Chen, P. Lin, Y. Yu, A. Wu, Biomed. Chromatogr. 21 (2007) 527–533.
[32] C. Sajeev, P.R. Jadhav, D. RaviShankar, R.N. Saha, Anal. Chim. Acta 463 (2002) 207–217.
[33] K.A.K. Musa, J.M. Matxain, L.A. Eriksson, J. Med. Chem. 50 (2007) 1735–1743.
[34] K.A.K. Musa, L.A. Eriksson, J. Phys. Chem. B 111 (2007) 13345–13352.
[35] D.A. Godwin, C.J. Wiley, L.A. Felton, Eur. J. Pharm. Biopharm. 62 (2006) 85–93.
[36] R. Dubakiene, M. Kupriene, Medicina 42 (2006) 619–624.
[37] S.D. Becke, J. Chem. Phys. 98 (1993) 5648–5652.
[38] C. Lee, W. Yang, R.G. Parr, Phys. Rev. B 37 (1988) 785–789.
[39] P.J. Stephens, F.J. Devlin, C.F. Chabalowski, M.J. Frisch, J. Phys. Chem. 98 (1994) 11623–11627.
[40] B. Mennucci, J. Tomasi, J. Chem. Phys. 106 (1997) 5151–5158.
[41] E. Cances, B. Mennucci, J. Tomasi, J. Chem. Phys. 107 (1997) 3032–3041.
[42] M. Cossi, G. Scalmani, N. Rega, V. Barone, J. Chem. Phys. 117 (2002) 43–54.
[43] M.E. Casida, in: D.P. Chong (Ed.), Recent Advances in Density Functional Methods, Pt. 1, World Scientific, Singapore, 1995, pp. 155–192.
[44] R.E. Stratmann, G.E. Scuseria, M.J. Frisch, J. Chem. Phys. 109 (1998) 8218–8224.
[45] M.E. Casida, C. Jamorski, K.C. Casida, D.R. Salahub, J. Chem. Phys. 108 (1998) 4439–4449.
[46] M.J. Frisch, G.W. Trucks, H.B. Schlegel, G.E. Scuseria, M.A. Robb, J.R. Cheeseman, J.A. Montgomery Jr., T. Vreven, K.N. Kudin, J.C. Burant, J.M. Millam, S.S. Iyengar, J. Tomasi, V. Barone, B. Mennucci, M. Cossi, G. Scalmani, N. Rega, G.A. Petersson, H. Nakatsuji, M. Hada, M. Ehara, K. Toyota, R. Fukuda, J. Hasegawa, M. Ishida, T. Nakajima, Y. Honda, O. Kitao, H. Nakai, M. Klene, X. Li, J.E. Knox, H.P. Hratchian, J.B. Cross, C. Adamo, J. Jaramillo, R. Gomperts, R.E. Stratmann, O. Yazyev, A.J. Austin, R. Cammi, C. Pomelli, J.W. Ochterski, P.Y. Ayala, K. Morokuma, G.A. Voth, P. Salvador, J.J. Dannenberg, V.G. Zakrzewski, S. Dapprich, A.D. Daniels, M.C. Strain, O. Farkas, D.K. Malick, A.D. Rabuck, K. Raghavachari, J.B. Foresman, J.V. Ortiz, Q. Cui, A.G. Baboul, S. Clifford, J. Cioslowski, B.B. Stefanov, G. Liu, A. Liashenko, P. Piskortz, I. Komaromi, R.L. Martin, D.J. Fox, T. Keith, M.A. Al-Laham, C.Y. Peng, A. Nanayakkara, M. Challacombe, P.M.W. Gill, B. Johnson, W. Chem, M.W. Wong, C. Gonzalez, J.A. Pople, Gaussian 03, Revision B.02, Gaussian, Inc., Wallingford, CT, 2004.
[47] J.J. Martinez-Pla, L. Escuder-Gilabert, S. Sagrado, R.M. Villanueva-Camanas, M.J. Medina-Hernandez, Internet Electron. J. Mol. Des. 4 (2005) 256–263.
[48] F. Yoshida, J.G. Topliss, J. Med. Chem. 43 (2000) 2575–2585.
[49] E.A. Lissi, M.V. Encinas, E. Lemp, M.A. Rubio, Chem. Rev. 93 (1993) 699–723.
[50] J. Llano, J. Raber, L.A. Eriksson, J. Photochem. Photobiol. A: Chem. 154 (2003) 235–243.